Electronic Supplementary Information (ESI)

Direct Imaging of Heteroatom Dopants in Catalytic Carbon Nano-Onions

Melonie P. Thomas,[#a] Namal Wanninayake,[#a] Manisha De Alwis Goonatilleke[a], Doo Young Kim,*[a] and Beth S. Guiton*[a]

[a] *Department of Chemistry, University of Kentucky, Lexington, Kentucky 40506, United States*

*: Corresponding authors: beth.guiton@uky.edu, dooyoung.kim@uky.edu

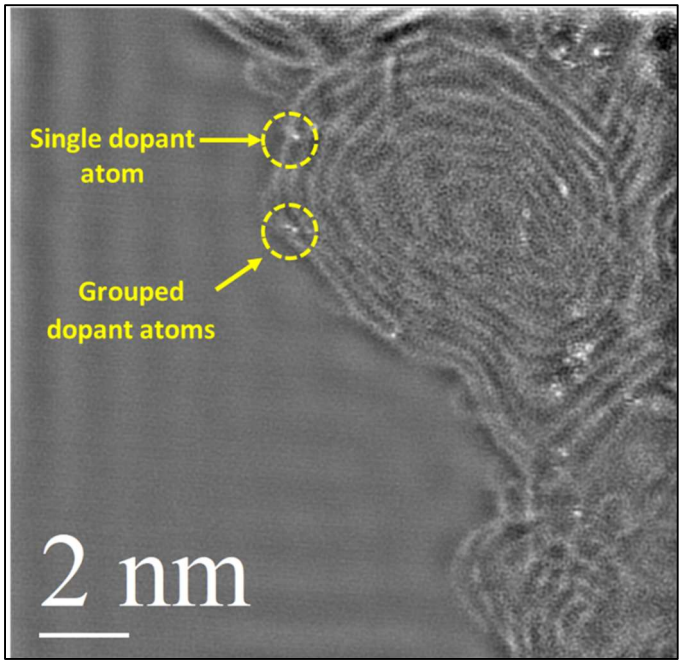

Figure S1. Fourier filtered HAADF image indicating single and grouped dopant atoms (yellow circles) in a N-CNO

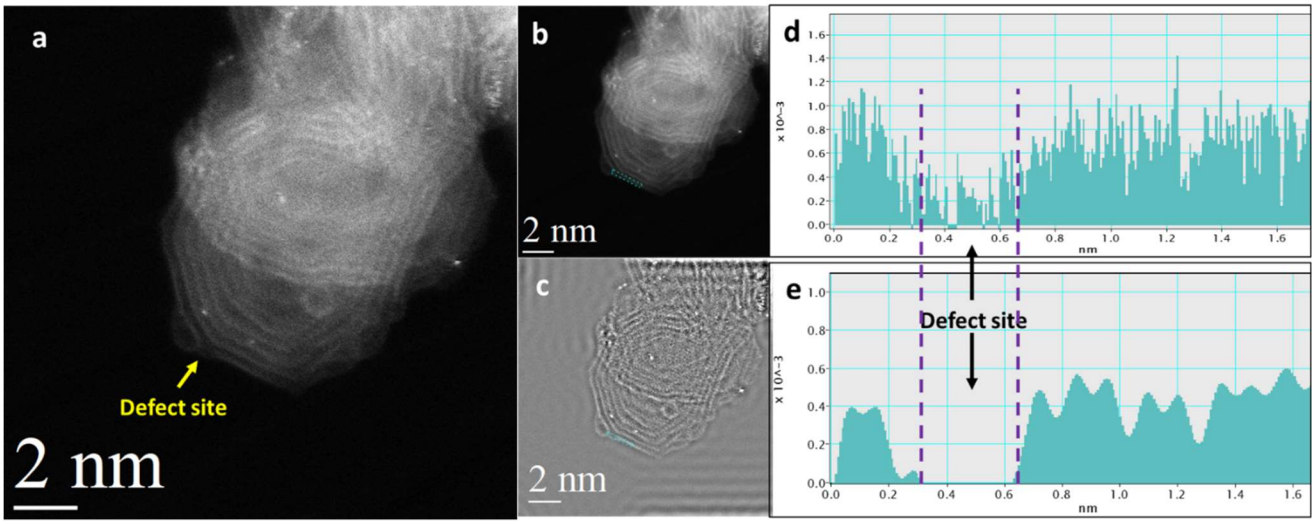

Figure S2. (a) HAADF micrograph showing the defect site in the outermost graphitic shell of a S-CNO, (b) indicates the position of the line profile (blue dashed box), (c) Fourier filtered image of (b) for improved clarity. (d) and (e) are line profiles across the defect sites in (b) and (c), respectively.

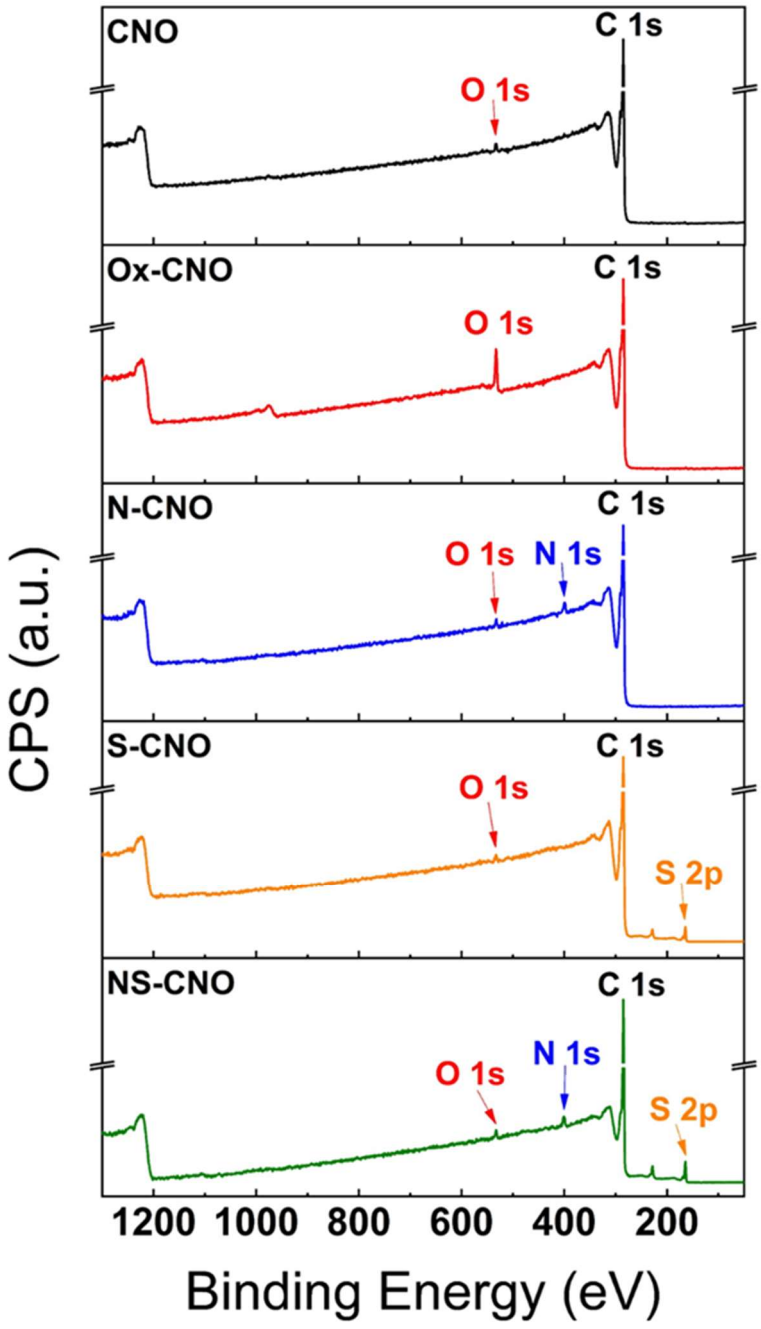

Figure S3. XPS survey scans of CNO, Ox-CNO, N-CNO, S-CNO and NS-CNO

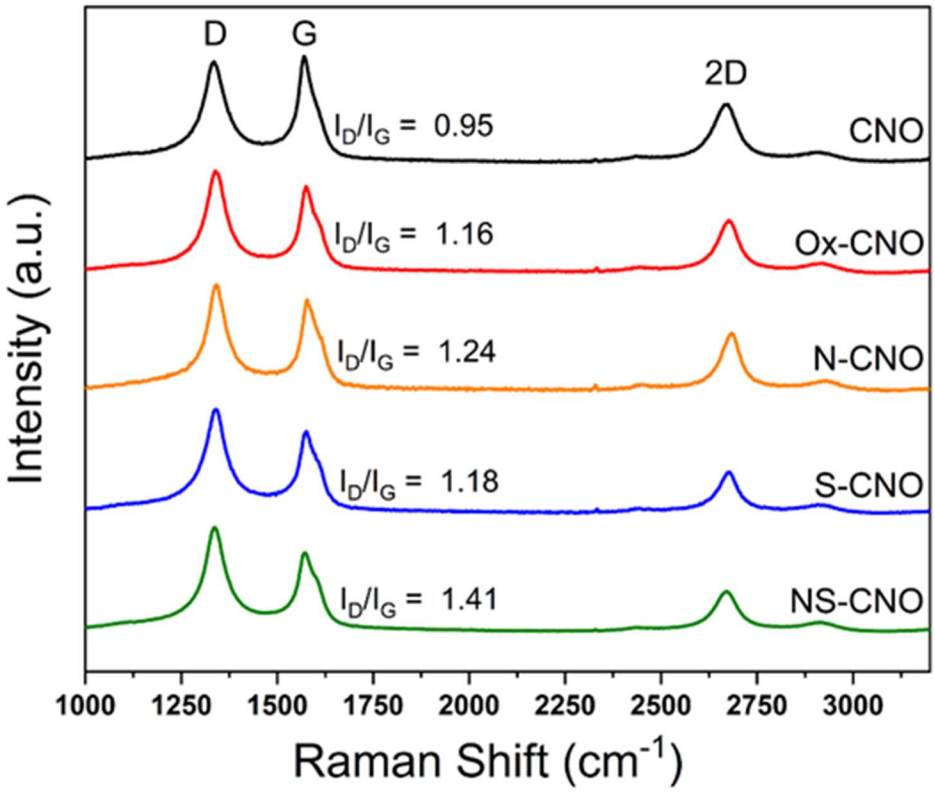

Figure S4. Raman spectra of CNO, Ox-CNO, N-CNO, S-CNO and NS-CNO

The first order G-band originates from the sp^2 hybridized (C-C) in-plane stretching mode for both rings and chains.[1] Typically, a G-band can be seen for all sp^2 hybridized systems.[2,3] It is noted that for all doped and undoped CNO samples, the G-band center is slightly downshifted (~1570 cm^{-1}) with respect to that of highly oriented pyrolytic graphite (~1580 cm^{-1}). This G-band downshift is attributed to the tensile strain in the graphene planes due to the curvature of the CNOs,[4] consistent with the curvature of the CNO remaining intact after doping. On the other hand, the first-order D-band arises from the breathing oscillation mode of sp^2 hybridized hexagonal C-C rings.[3] This vibrational mode becomes active only in the presence of symmetry breaking defects such as heteroatoms, vacancies, sp^3 centers and grain boundaries.[2] The intensity ratio, I_D/I_G, is therefore a measurement of the material disorder.[5]

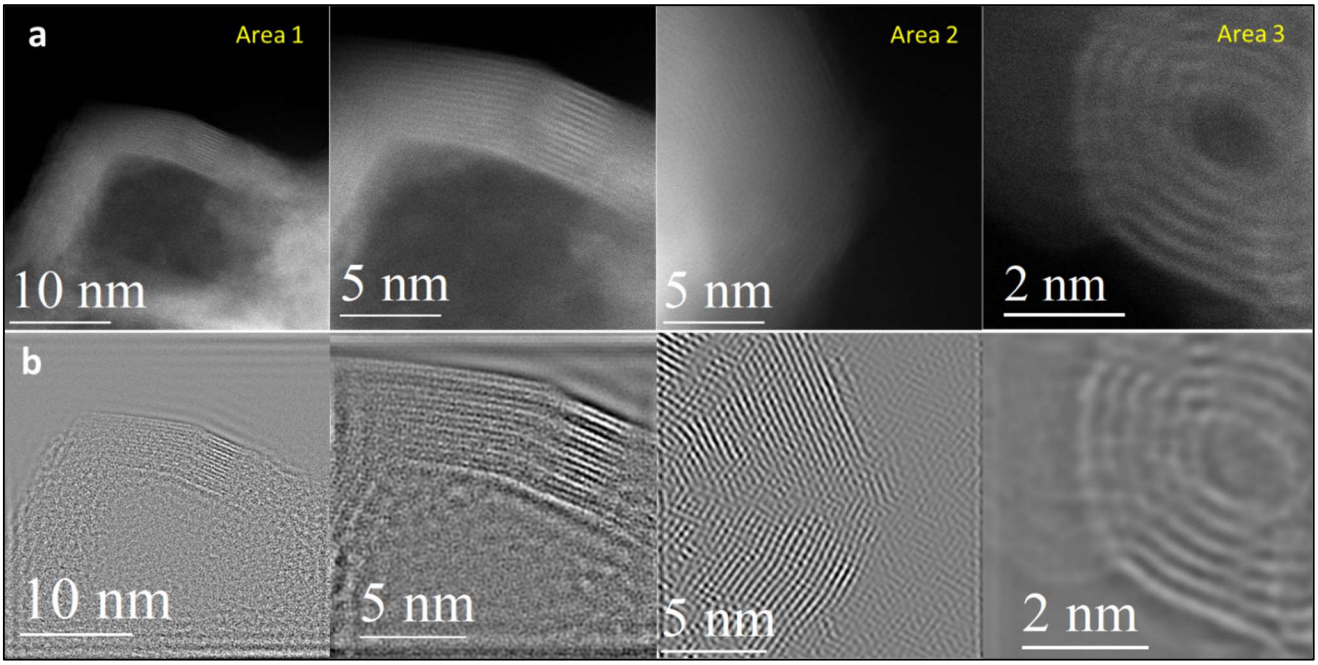

Figure S5. (a) HAADF micrographs and (b) the respective Fourier filtered images of pristine CNOs imaged at three different areas of the same sample.

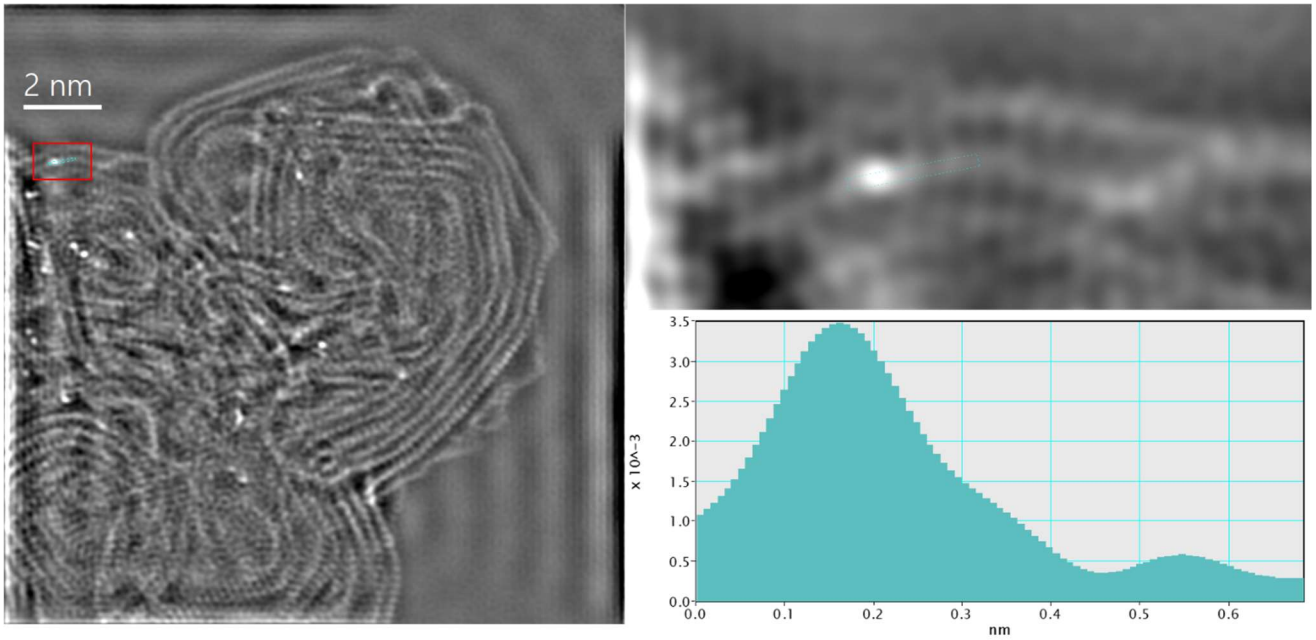

Figure S6. Line scan across C and S atoms in S-CNO sample (HAADF image)

The scattering intensity of electrons on this detector $\propto Z^{1.6\text{-}1.9}$

Intensity ratio (from HAADF micrograph (Figure S1) = $\frac{3.5\ x\ 10^{-3}}{0.5\ x\ 10^{-3}} = 7$

Ratio between $Z^{1.9}$ of S and C = $\frac{16^{1.9}}{6^{1.9}} = 6.45$

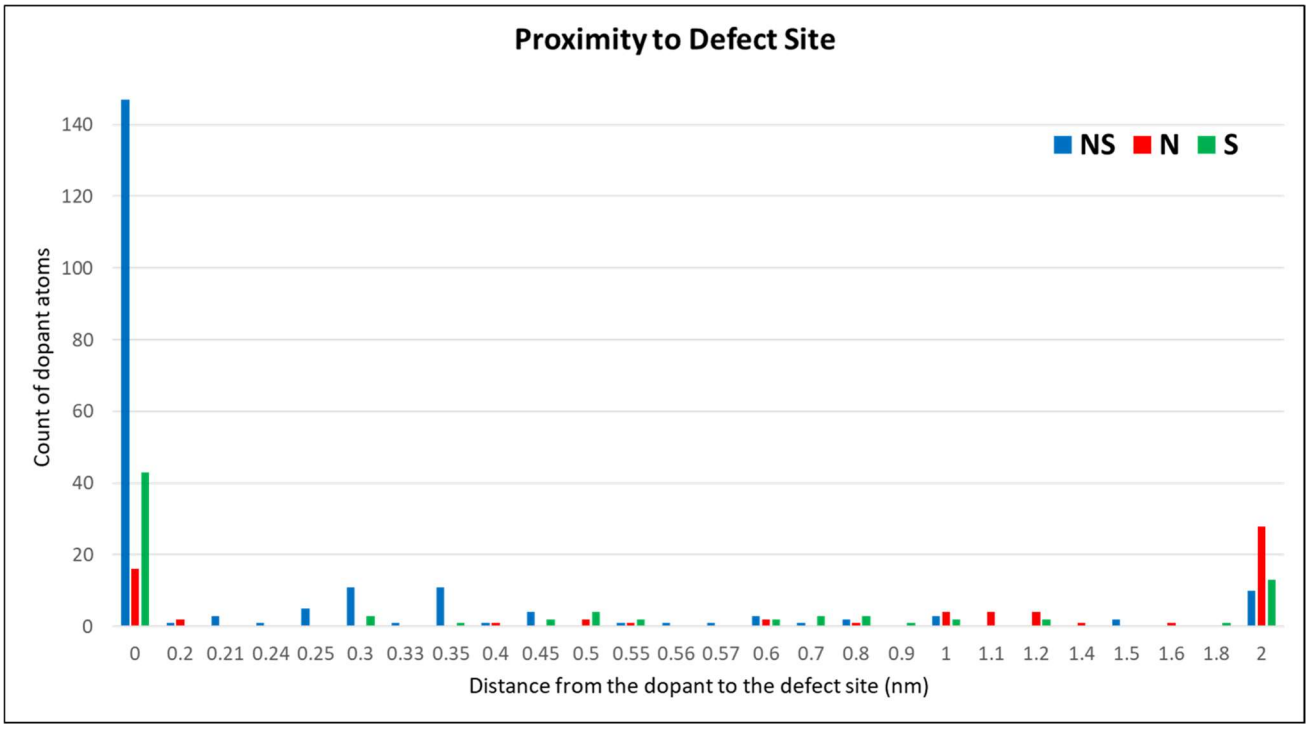

Figure S7. Proximity to defect site histogram with equal bin size (0.01 nm).

Table S1. Quantitative analysis of NS-CNO

	Dopant atom				Proximity to defect site									
CNO	Single	Grouped			At defect site				0 - 0.4 nm		0.41- 0.7 nm		>0.71nm	
	1	2	3	4	1	2	3	4	Number of dopants	Proximity (nm)	Number of dopants	Proximity (nm)	Number of dopants	Proximity (nm)
1	3				2								1	1.00
2	2												1	0.80
													1	>2.0
3	3		1						3	0.35	1	0.45		
									1	0.25				
									1	0.35				
4	3	1	1		1		1		1	0.24			1	> 2.0
													2	1.50
5	9	3	2		7	2	1		1	0.30				
									1	0.35				
									3	0.21			2	>2.0
6	5	1	1	1	1	1	1	1	1	0.35	1	0.55		
											1	0.57		
											1	0.56		
7	8	2			6	2			1	0.33	1	0.45		
8	7	1			4	1			1	0.40				
									1	0.35				
									1	0.25				
9	8	3			7	2			1	0.20				
									2	0.30				
10	6	4			3	3			1	0.35	1	0.45		
									1	0.30				
									2	0.30				
11-12	11	2	1	1	9	2	1	1	1	0.25			1	>2.0
13-14	7		1		4		1				1	0.45	1	>2.0
													1	0.80

15	3	1			1	1			1	0.25				
									1	0.35				
16	2				2									
17	2				1				1	0.30				
18-21	10	2			7	2			1	0.30	1	0.60		
									1	0.30				
22-23	3				2								1	1.10
24-29	9		1	1	7		1	1			1	0.70	1	1.00
30-32	6	1			6						2	0.60		
33-36	7	1	1		5	1			1	0.35			1	2.00
													3	>2.0
37-39	7	1	1		5		1		1	0.35				
									2	0.30				
									1	0.25				

Table S2. Quantitative analysis of S-CNO

	Dopant atom				Proximity to defect site									
CNO	Single	Grouped			At defect site				0 - 0.4 nm		0.41- 0.7 nm		>0.71nm	
	1	2	3	4	1	2	3	4	Number of dopants	Proximity (nm)	Number of dopants	Proximity (nm)	Number of dopants	Proximity (nm)
1-4	12				8						1	0.45	1	0.9
											1	0.6	1	0.8
5-7	5	4	1		1	3	1		1	0.3	1	0.7		
											2	0.55		
											1	0.6		
											1	0.45		
8-10	2	1	1	1		1	1				4	0.5	1	>2.0
													1	>2.0
11-16	5	2			2	2							1	>2.0
													1	1.2
													1	0.8
17-24	10		1		2		1		1	0.3	1	0.7	1	1
									1	0.3			1	1
													1	0.8
													1	>2.0
													1	1.8
25-27	12				7								1	1.2
													1	>2.0
													1	>2.0
													1	>2.0
													1	>2.0
28-29	9								1	0.35	1	0.7	1	>2.0
													1	>2.0
													1	>2.0
													1	>2.0
													1	>2.0

Table S3. Quantitative analysis of N-CNO

CNO	Dopant atom				Proximity to defect site									
	Single	Grouped			At defect site				0 - 0.4 nm		0.41- 0.7 nm		>0.71nm	
	1	2	3	4	1	2	3	4	Number of dopants	Proximity (nm)	Number of dopants	Proximity (nm)	Number of dopants	Proximity (nm)
1-4	4										1	0.50	1	1.60
													1	1.10
													1	0.80
5-9	6	2			1	1					1	0.55	1	1.40
													1	1.00
													1	1.10
													2	>2.0
													1	>2.0
10-12	7	2			2				2	0.20	1	0.60	1	>2.0
									1	0.40			1	>2.0
													2	1.10
													1	>2.0
13-22	10	2	3		4	1	1						1	1.20
													1	1.20
													3	>2.0
													1	>2.0
													2	1.20
													1	>2.0
													1	>2.0
													3	1.00
													1	>2.0
23-24	4				1						1	0.60	1	>2.0
													1	>2.0
25-27	5	1	1		1						1	0.50	1	>2.0
													1	>2.0
													3	>2.0
													2	>2.0
													1	>2.0
28-30	3	1											1	>2.0
													1	>2.0
													1	>2.0
													2	>2.0

Table S4. Results of XPS survey scans

Sample	C 1s (at. %)	O 1s (at. %)	N 1s (at. %)	S 2p (at. %)
CNO	99.17 ± 0.24	0.83 ± 0.18		
Ox-CNO	93.95 ± 0.40	6.05 ± 0.34		
N-CNO	96.81 ± 0.35	1.01 ± 0.21	2.18 ± 0.09	
S-CNO	97.01 ± 0.50	0.97 ± 0.25		2.02 ± 0.17
NS-CNO	94.55 ± 0.45	1.12 ± 0.18	2.19 ± 0.12	2.14 ± 0.14

n=3

Initial oxidation of CNO increases oxygen functional groups and subsequent heteroatom doping reduces the oxygen content due to the exchange of heteroatoms or due to the removal of oxygen during the thermal annealing. It is important to mention that, after doping, the heteroatom content of each sample is approximately twice that of oxygen (Table S4).

References

1 A. C. Ferrari and D. M. Basko, *Nature Nanotechnology*, 2013, **8**, 235–246.

2 R. Beams, L. G. Cançado and L. Novotny, *J. Phys.: Condens. Matter*, 2015, **27**, 083002.

3 R. Krishna, A. N. Jones, L. McDermott and B. J. Marsden, *Journal of Nuclear Materials*, 2015, **467**, 557–565.

4 D. Roy, M. Chhowalla, H. Wang, N. Sano, I. Alexandrou, T. W. Clyne and G. A. J. Amaratunga, *Chemical Physics Letters*, 2003, **373**, 52–56.

5 L. G. Cançado, A. Jorio, E. H. M. Ferreira, F. Stavale, C. A. Achete, R. B. Capaz, M. V. O. Moutinho, A. Lombardo, T. S. Kulmala and A. C. Ferrari, *Nano Lett.*, 2011, **11**, 3190–3196.